J. Fish. Sci. Tech. 5(1), 5~20, 2002

JOURNAL OF
FISHERIES SCIENCE
AND TECHNOLOGY

Hydraulic Model Experiment on the Circulation in Sagami Bay, Japan (II)

– Dependence of the Circulation Pattern on External and Internal Rossby Number in Baroclinic Rotating Model –

Hyo-Sang Choo* and Takasige Sugimoto[1]

**Dept. of Oceanography, Yosu National Univ., Yeosu 550-749, Korea*
[1]Ocean Research Institute, Univ. of Tokyo, Tokyo 164-8639, Japan

(Received July 2001, Accepted February 2002)

To investigate the effect of mechanical parameters on the circulation and its fluctuation in Sagami Bay, baroclinic model experiments were carried out by use of a two-layer source-sink flow in a rotating tank. In the experiment, a simple coastal topography with flat bottom was reproduced. The results show that the path of the Through Flow, which corresponds to the branch current of the Kuroshio, depends on external Rossby number (Ro) and internal Rossby number (Ro*), and divided into two regimes. For Ro*≤1.0 in which Rossby internal radius of deformation of the Through Flow is smaller than the width of the approaching channel, the current flows along the Oshima Island as a coastal boundary density current separated from the western boundary of the channel. For Ro*>1.0, it changes to a jet flow along the western boundary of the channel, separated from the coast of Oshima Island. The current is independent on both Ro and Ro* in the regime of Ro*>1.0, Ro≥0.06 and Ro*≤1.0, Ro≥0.06. The pattern of the cyclonic circulation in the inner part of the bay is also determined by Ro and Ro*. In case of Ro*≤1.0, frontal eddies are formed in the northern boundary of the Through Flow. These frontal eddies intrude into the inner part along the eastern boundary of the bay providing vorticity to form and maintain the inner cyclonic circulation. For Ro*>1.0, the wakes from the Izu peninsula are superposed intensifying the cyclonic circulation. The pattern of the cyclonic circulation is divided into three types; 1) weak cyclonic circulation and the inner anticyclonic circulation (Ro<0.12). 2) cyclonic circulation in the bay (0.12≤Ro<0.25). 3) cyclonic circulation with strong boundary current (Ro≥0.25).

Key words: Hydraulic Model, Baroclinic two-layer source-sink flow, Kuroshio, Through Flow, Rossby number, Cyclonic circulation, Frontal eddies, Wakes

Introduction

Dynamics of the circulation and its fluctuation in Sagami Bay were investigated by use of a rotating tank. Fig. 1 shows the topography of Sagami Bay, which has the width of about 80 km and the length of 57 km. The mouth of the bay is divided into two parts, Oshima Western and Oshima Eastern Channel, by Oshima Island. The width of Oshima Western Channel is about 21 km and its maximum depth at the sill is about 600 m. While, Oshima Eastern Channel is about 2,000 m in depth and 37 km in width. In Sagami Bay, there exists a branch of the Kuroshio, namely a Through Flow, which enters mostly from the Oshima Western Channel and flows out through Oshima Eastern Channel. The circulation in Sagami Bay is strongly governed by the fluctuation of this Through Flow.

Uda (1937) proposed the average flow pattern of Sagami Bay based on the hydrographic field observation. While, Kimura (1942) investigated an intermittent rapid intrusion of oceanic warm water called "Kyucho" which are indicated by stepwise rise of the coastal water temperature. Since then,

*Corresponding author: choo@yosu.ac.kr

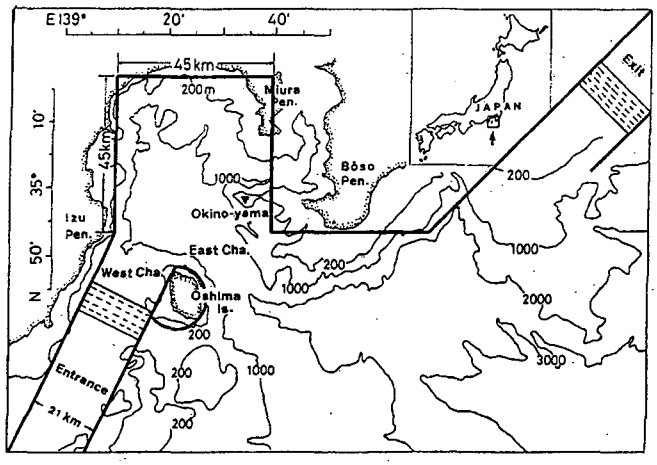

Fig. 1. Domain of the hydraulic model and the general configuration. Thick lines indicate the complete boundary of the model. Thin lines show bathymetry of the prototype Sagami Bay and the dimension of the depth is meter.

many field studies on the circulation and its fluctuation in Sagami Bay were made. Kimura (1942), Yoshida (1960) and Kawata and Iwata (1957) confirmed the existence of the Through Flow as a branched current and the cyclonic circulation in the inner part of the bay based on the observations with drifting buoys, GEK and moored current meters, respectively. Momoi (1976) also examined the cyclonic circulation in Sagami Bay by the analysis of ten years GEK data. Iwata (1986) carried out surface current observations by use of mooring systems at the inner shelf and the slope areas less than 500 m depth and indicated that the intensity of the circulation current velocity over the Okinoyama Bank off the southern tip of Miura Peninsula were well correlated with the cyclonic circulation in the inner part of the bay. Also, it was found that currents running parallel to the coast showed fluctuations with 3~6 day and 9 day periods. Iwata (1986) estimated the intensity of the Through Flow by using the latitude of the Kuroshio axis or the sea level change in Miyake Island. While, Odamaki (1991) pointed out that when the Kuroshio path located quite away from Sagami Bay the Through Flow took place from Oshima Eastern Channel. Iwata and Matsuyama (1989) and Hasunuma et al. (1983) reviewed the circulation patterns in Sagami Bay by use of moored current meters and drifting buoys. On the other hand, Tameishi (1988) showed similar variations in circulation patterns in relation to the Kuroshio path off Sagami Bay by using NOAA infrared images. Field observations on the circulation in Sagami Bay obtained up to the present by using drifting buoys and moored current meters are shown in Fig. 2. The flow pattern in Fig. 2 was drawn by the observational results for the case of a large volume transport of the Through Flow.

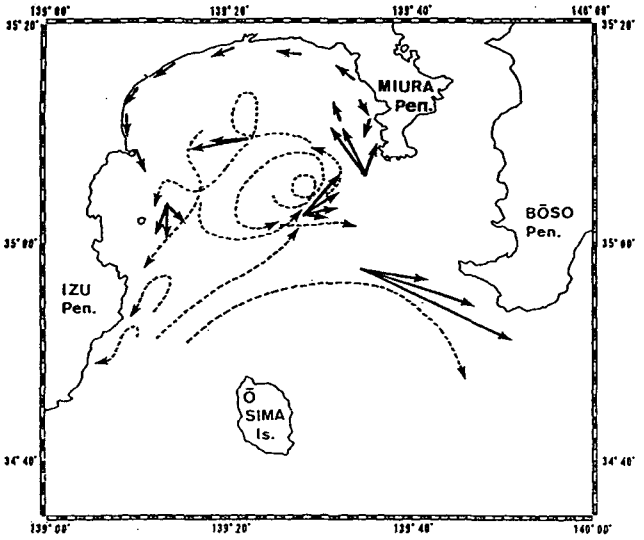

Fig. 2. The observational results of current meters and drifting buoys in Sagami Bay. The arrows of solid line indicate current vectors during 1982~1983 and the dashed lines are paths of the drifting buoys tracked during Mar. 1979 (after Iwata and Matsuyama, 1989; Nakada et al., 1989).

However, the dynamics of the circulation and its fluctuations are still remained unsolved, which are 1) the quantitative relationship between the volume transport of the Through Flow and the latitudinal positions of Kuroshio path off Sagami Bay, 2) the behavior of the Through Flow in Sagami Bay and Oshima Eastern Channel including the wake in the northeast of Oshima Island, 3) effects of the Through Flow on oceanographic condition and currents on the continental shelf in Sagami Bay.

To investigate the mechanics of the circulation and its fluctuation in Sagami Bay, Choo and Sugi-

moto (1992) studied the dependence of the circulation pattern on Reynolds number, Rossby number and the inflow-outflow conditions (angles) by use of a barotropic rotating model. As to two-layer model experiments on the dynamics of outflow from the straits, Nof (1978) investigated effects of thickness of the entrance channel and horizontal shear of the inflow on the flow pattern of the outflow from a channel. For the flow pattern of light water through a channel, Whitehead and Miller (1979) showed that anticyclonic warm water eddies were formed when the Rossby radius of deformation was greater than the radius of curvature of the coast line. Kawasaki and Sugimoto (1984) analyzed the shape of Tsugaru warm current by using non-dimensional parameters. They discussed the relative importance of the bottom topography and the inertial term in rotating fluid for coastal mode. Also the short-term fluctuations of Tsugaru Warm Water eddy were examined with the change of flow rate (Kawasaki and Sugimoto, 1988).

Another studies on the two-layer model experiments are about coastal boundary density currents and frontal waves. Vinger and McClimans (1980) indicated that the growing feature of the frontal wave was able to be classified by internal Froude number ($V/(g'h)^{1/2}=1.0$, where g' is reduced gravity) in their source-sink flow model experiment for the coastal density current. Stern et al. (1982) showed that eddy rows were formed at the density front caused by the flow of low density water and this process had a close relationship with the conservation of potential vorticity. Kubokawa and Hanawa (1984) presented that a quasi-geostrophic frontal wave is formed by the intrusion of the density current and calculated its propagation speed. However, in order to make clear the connection of these experimental results with the circulation structure and to realize the mechanics of the circulation and its fluctuation in Sagami Bay, it is necessary to carry out a hydraulic model experiment for Sagami Bay.

In this study, the relationship between the Through Flow path and the formation of the cyclonic circulation in Sagami Bay were examined by hydraulic two-layer model experiments. A source-sink flow model was used on a rotating table and the dependency of the current path and the circulation pattern on relevant physical parameters is investigated.

Models and Experimental Arrangements

1. Description of dynamical balance of circulations

The Through Flow in Sagami Bay flows with anticyclonic curvature and is known as a gradient flow, in which pressure gradient force are balanced by Coriolis force with the centrifugal force being about 50 percents of the Coriolis force (Taira et al., 1987). The depth of the Through Flow (H) which is calculated by dividing the mass transports per unit width of main current M (100~300 m^2/s) by average surface current speeds V (0.5~1.0 m/s) is 200~300 m and the thickness of the flow is sufficiently deep compared with the bottom Ekman depth ($(K_z/f)^{1/2}$ is 1~10 m, where K_z is assumed $1\sim10^2$ cm^2/s). North-south change of the Coriolis parameter, about 4×10^{-7} (c.g.s) is negligibly small in comparison with the curvature variation in vorticity V/Rc (2.0×10^{-5} (c.g.s), where V is mean current speed (~50 cm/s), Rc a radius of curvature (~25 km)) of the Through Flow. Assuming the value of K_h is 1.8×10^5 cm^2/s, the magnitude of the horizontal eddy Reynolds number Reh (VL/K_h) is greater than $1\sim10^3$. Hence, the effect of viscosity in the momentum balance is considered very small. However, it is considered that the cyclonic vorticity near the northern boundary of the Through Flow as well as the coastal boundary current are important in the formation of the inner cyclonic circulation (Choo and Sugimoto, 1992).

In this study, non-dimensional parameter analyses were carried out to study the dynamics of the Through Flow and the circulation in Sagami Bay based on the result of an upper layer source-sink flow model in a rotating tank. Dependence of the Through Flow and circulation on non-dimensional parameters, such as internal Rossby number Ro* ($(g'H)^{1/2}/fB$), where B is the width of the approaching channel and external Rossby number Ro (V_0/fL, where L is the width of the bay), was investigated in our hydraulic two-layer model experiments.

2. Basic equations and similitude

In order to simulate the circulation in Sagami Bay, a stably stratified two-layer with stagnant lower

layer was assumed. Then the equation of motion for the upper layer is expressed by

$$\partial V/\partial t+V\cdot\nabla V+f\,k\times V=-g'\nabla h+K_h\nabla^2V+K_z\partial^2V/\partial Z^2 \quad (1)$$

where V is the horizontal velocity vector of the upper layer, t is time, $\nabla=\partial/\partial x\,i+\partial/\partial y\,j$, $\nabla^2=\partial^2/\partial x^2+\partial^2/\partial y^2$, h the thickness of the upper layer in the prototype, f the Coriolis parameter, k the unit vector of the upward component, g′ reduced gravity $=(\Delta\rho/\rho)g$ (g is gravity, $\Delta\rho$ is density difference between the upper and lower layer), K_h and K_z the horizontal and vertical eddy viscosity, respectively.

Equation (1) for the prototype can be scaled with the typical horizontal length scale L (the width of Sagami Bay~45 km), the typical time scale f^{-1}, the characteristic speed of the current V_0 (horizontal velocity of the Through Flow), the characteristic upper layer depth H (an average thickness of upper layer~200 m). Then it becomes

$$\partial V^*/\partial t^*+Ro\cdot V^*\cdot\nabla^*V^*+k\times V^*=(Ro//Fr_i^2)\cdot\nabla^*h^*+Ek_h\cdot\nabla^{*2}V^*+Ek_z\cdot\partial^2V^*/\partial Z^{*2} \quad (2)$$

where asterisks means non-dimensional variables and Ro, Fr_i, Ekh and Ek_z are external Rossby number (V_0/fL), internal Froude number $(V_0/(g'H)^{1/2})$, horizontal Ekman number (K_h/fL^2) and vertical Ekman number (K_z/fH^2), respectively. Using the value $K_h\sim1.8\times10^5$ cm²/s and $K_z\sim2.6\times10$ cm²/s (Sugimoto, 1977), the values of non-dimensional parameters in equation (2) become $Ro\sim10^{-1}$, $Fr_i\sim10^{-1}$, $Ro/Fr_i\sim1$, $Ek_h\sim10^{-4}$ and $Ek_z\sim10^{-4}$ as shown in Table 1. If the four parameters Ro, Fr_i, Ek_h and Ek_z are made equal between the prototype and the model, the flow patterns as a solution of equation (2) become equivalent between the prototype and the model. Then the similitude of these four parameters between the prototype and the model are expressed as follows.

$$[V_0/fL]_p=[V_0/2\Omega L]_m \quad (3)$$
$$[V_0/(g'H)^{1/2}]_p=[V_0/(g'H)^{1/2}]_m \quad (4)$$
$$[K_h/fL^2]_p=[\nu/2\Omega L^2]_m \quad (5)$$
$$[K_z/fH^2]_p=[\nu/2\Omega H^2]_m \quad (6)$$

where ν is the molecular viscosity, Ω the angular velocity of the turn table and the subscript p and m denote prototype and model, respectively. Then denoting the model-to-prototype ratio by subscript r, it follows that

$$V_r=L_r/T_r \quad (7)$$
$$V_r^2=H_r \quad (8)$$
$$K_{hr}=L_r^2/T_r \quad (9)$$
$$K_{zr}=H_r^2/T_r \quad (10)$$

where V_r, L_r, T_r, H_r, K_{hr} and K_{zr} represent $V_r=(V_0)_p/(V_0)_m$, $L_r=(L)_p/(L)_m$, $T_r=f/2\Omega$, $H_r=(H)_p/(H)_m$, $K_{hr}=(K_h)_p/(\nu)_m$ and $K_{zr}=(K_z)_p/(\nu)_m$ respectively. In our two-layer model, as external Rossby number Ro and internal Rossby number Ro* (Ro/Fr_i) are much greater than horizontal Ekman number Ek_h and vertical Ekman number Ek_z it is assumed that the conditions of the model ratios by Ro or Ro* are primarily important. Therefore, the relation $L_r=T_r$ $H_r^{1/2}$ from equation (7) and (8) become the most important condition on determining the ratios of the model. A typical set of these scale ratios is listed in Table 1 with the representative values of the properties in the prototype and the model. The mean upper layer water depth of the model used was 5.5 cm corresponding to the upper layer depth of 200 m in the prototype.

Table 1. Scale ratios of the model and the values of parameters for the prototype and the model

Property		Scale ratio	Prototype	Model
Horizontal length	L	$L_r=3.0\times10^5$	45 km	15 cm
Vertical length	H	$H_r=3.6\times10^3$	1,000 m	28 cm
Time	T	$T_r=5.0\times10^3$	1.5×10^5 sec	30 sec
Volume transport	Q	$Q_r=6.5\times10^{10}$	2.0×10^{12} cm³/s	30 cm³/s
Velocity	V	$V_r=6.0\times10^1$	60 cm/s	1.0 cm/s
Kinematic	K_h	$K_{hr}=1.8\times10^7$	1.8×10^5 cm²/s	0.01 cm²/s
Viscosity	K_z	$K_{zr}=2.6\times10^3$	2.6×10^1 cm²/s	0.01 cm²/s

3. Experimental facilities and procedure

A turn table (1.2 m in diameter) was driven with a synchronous induction motor at a constant rate of an accuracy of 0.5%. The model basin, with its height 35 cm, width 120 cm and length 80 cm was made of plexiglass of 0.5 cm thickness. Thick lines in Fig. 1 indicate the complete boundary of the model. Fig. 3(a) and (b) show the side view of the model, its outside arrangement and the measurement system. To eliminate the influence of the air flow outside, the tank was covered with a clear flat plexiglass plate, containing the air layer between the plate and the water surface. Room temperature was controlled within 1℃.

The flow in the model was driven by a source-

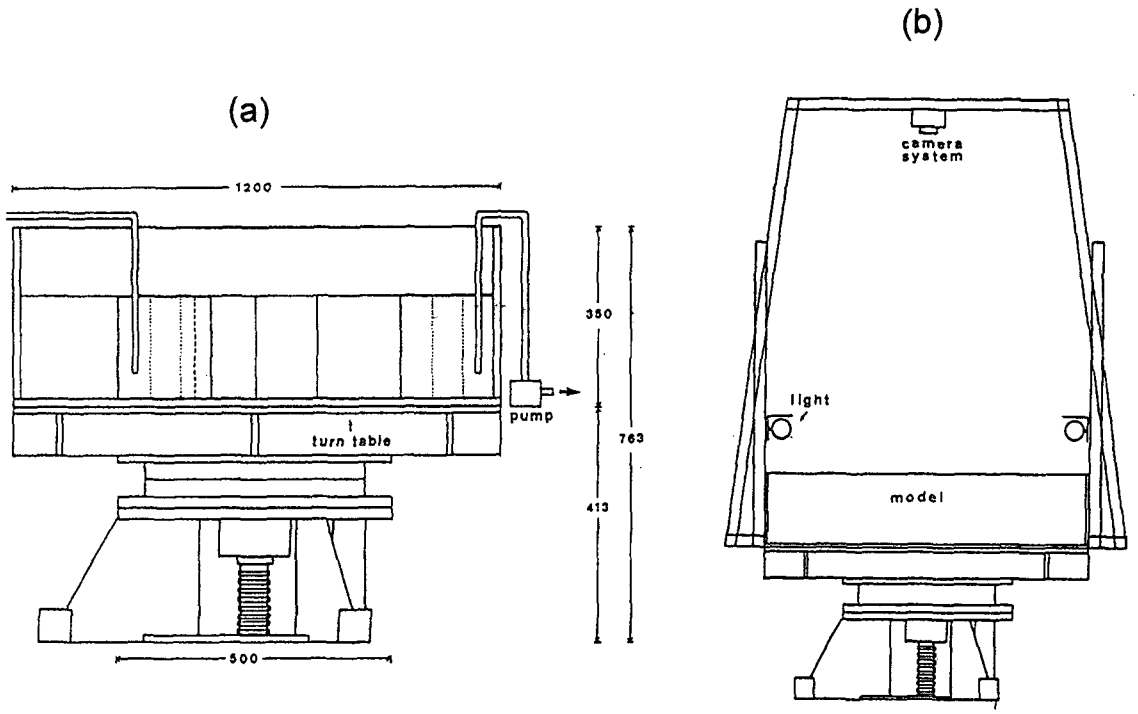

Fig. 3. (a) Schematic views of the turntable, the tank and (b) the measurement system in the model experiment. All dimensions are given in millimeters.

sink system by use of an electro-magnetic pump. The volume transport was measured by a floater-type flow meter (maximum 200 liters/hr) with an error of a few percent in a flow rate. Turbulence from the source and the sink was reduced by screens, seven sheets of iron nets with 1.5 mm mesh size and two sheets of sponges with 5 mm thickness. It was found that the flows passing through the screens in the approaching channel were almost uniform. Effect of the surface film was reduced by filtering the working fluid before the experiment. In our model the depths of the upper and the lower layer were set up 5.5 cm and 17 cm (three times deeper than the upper layer) and only the low density water of the upper layer was driven. Fig. 4 shows the length sectional view of the approaching channel.

The processes of two-layer model experiments were as follows. At the beginning, the density controlled salty water were filled up in the lower layer of the model. Then, through the approaching channel shown in Fig. 4, the upper pure water were poured into above the lower salty water with calm. After the upper pure water was approached at 5.5 cm depth, the working fluid becomes the state of

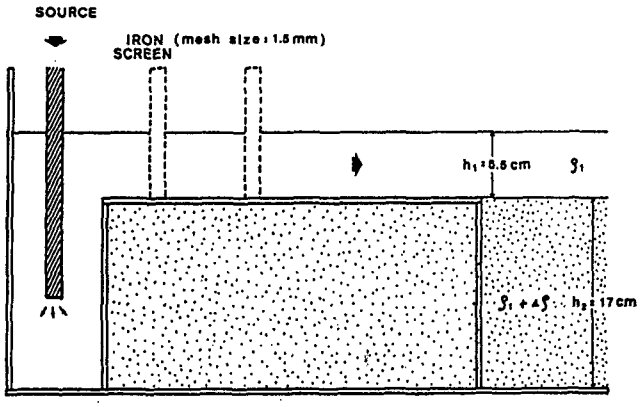

Fig. 4. A side view in along-stream direction of the entrance channel in two layer model experiment.

rigid body rotation by rotating the model. The upper pure water was injected to the upper layer of the model from the source in the approaching channel and discharged into the sink in the exit channel with a fixed flow rate of the source-sink system.

In experiment spin-up time of the upper pure water is $(H/\delta_{\cdot E})\Omega^{-1}\sim 3$ minute, where $\delta_{\cdot E}((\nu/\Omega)^{1/2}\sim$ 0.2 cm) is the depth of Ekman mixed boundary layer. More than 3 minutes were given for the upper pure water to spin-up in rotation. After the fluid

flow was in quasi-steady state, the current was measured. The time to take measures was within 5 minutes. During this process, it was assumed that density change in the upper and the lower layer by vertical mixing was small.

The current was determined by use of photography and video tapes coupled with two types of flow visualization; (1) To determine the flow pattern, aluminum flakes were placed on the surface and photographed with a time-lapse still camera and/or a video camera. The flows were analyzed and drawn from photographs and motion pictures. These pictures show fine structures and transitory eddies in addition to the major circulation pattern. To prevent the contamination of the flakes, a photo-flo solution was added in the fluid. (2) To obtain the lateral velocity profiles at the entrance and the interior regions, thymol blue dye technique was used. A normal NaOH solution was also introduced continuously from a blood transfusion syringe at the inlet to make streamlines of tracers. A video camera was mounted on a frame attached to the rotating table and operated with remote control switches (Fig. 3).

It is shown that density difference between the Through Flow for the upper layer and the subarctic intermediate water in Sagami Bay for lower layer is about 1.5×10^{-3} for yearly mean and fluctuates from 1.7×10^{-3} (in winter) to 5.0×10^{-3} (in summer) (Iwata, 1979). Then in our model experiment the cases of density differences were based on these observational results. Standard cases of model experiments were deployed as the following fixed parameters $\Delta\rho=1.5\times10^{-3}$, $\Omega=2$ rpm. Parameter ranges are listed in Table 2. The flow rate Q has a range of $5.5\sim56.0\ cm^3s^{-1}$.

Results

1. Path of the Through Flow

Fig. 5(a), (b) and (c) show the flow patterns of the Through Flow for the standard flow rates with density differences of $\Delta\rho=5.0\times10^{-4}$, 1.5×10^{-3} and 5.0×10^{-3}, respectively. Corresponding internal Rossby radius of deformation (Rd) are 3.9 cm, 6.8 cm and 12.4 cm (in the prototype 11.7 km, 20.4 km and 37.2 km), respectively. Five lines in each figure indicate the outer (northern) edge of the Through Flow for the flow rate $Q=5.5\ cm^3s^{-1}$, $14.0\ cm^3s^{-1}$, $27.0\ cm^3s^{-1}$, $42.0\ cm^3s^{-1}$ and $56.0\ cm^3s^{-1}$. For $\Delta\rho=5.0\times10^{-4}$ and 1.5×10^{-3}, the width of the Through Flow ($\sim$ Rd) is smaller than the breadth of the approaching channel (B=7 cm). In Fig. 5(a) and (b), the current flows with a shape of loop and its path proceeds northward with the increase of flow rates. For $\Delta\rho=5.0\times10^{-3}$ (Fig. 5(c)) as Rd is larger than B, the current flows in contact with the left-hand side boundary of the approaching channel. The current path in the bay proceeds furthest northward for the smallest flow rate ($Q=5.5\ cm^3s^{-1}$) and retreats toward Oshima Island with the increase of flow rate.

The dependence of northward penetration length rate lp/L of the Through Flow on Ro* for the experimental cases is shown in Fig. 6(a), (b) and (c), where lp represents the northward penetration length of the Through Flow reached from the northern edge of Oshima Island to the northward outer edge of the Through Flow (Fig. 5(c)) and L represents the horizontal length of the bay. The dotted and solid lines in the figures show contours of internal Rossby number Ro* and northward penetration length rate of the Through Flow lp/L, respectively. Volume transports in Fig. 6(a), (b) and (c) are $Q=5.5\ cm^3s^{-1}$, $Q=27.0\ cm^3s^{-1}$ and $Q=56.0\ cm^3s^{-1}$, respectively. Internal Froude number Fri that is measured by density difference and volume transport ranges $1.2\times10^{-2}\sim2.7\times10^{-2}$, $6.0\times10^{-2}\sim1.35$ and $1.3\times10^{-1}\sim2.89$ in Fig. 6(a), (b) and (c), respectively.

For Fri$\ll$1.0 (Fig. 6(a)), lp/L changes from 5.0×10^{-2} to 3.5×10^{-1}. Lp/L increases $5.0\times10^{-2}\sim1.5\times10^{-1}$

Table 2. Cases and parameter ranges of the baroclinic model experiment

Factors		Values given in the model									
Density difference	$\Delta\rho$	0.00005		0.0005		0.0015		0.005		0.025	
Revolution rate	Ω(rpm)	1/2				2				4	
Volume transport	Q(cm^3/s)	5.5	8.3*	11.1*	14.0	20.8*	27.0	34.7*	42.0	48.6*	56.0

*$\Delta\rho$=0.00005, 0.0015, 0.025 only; __ Standard case.

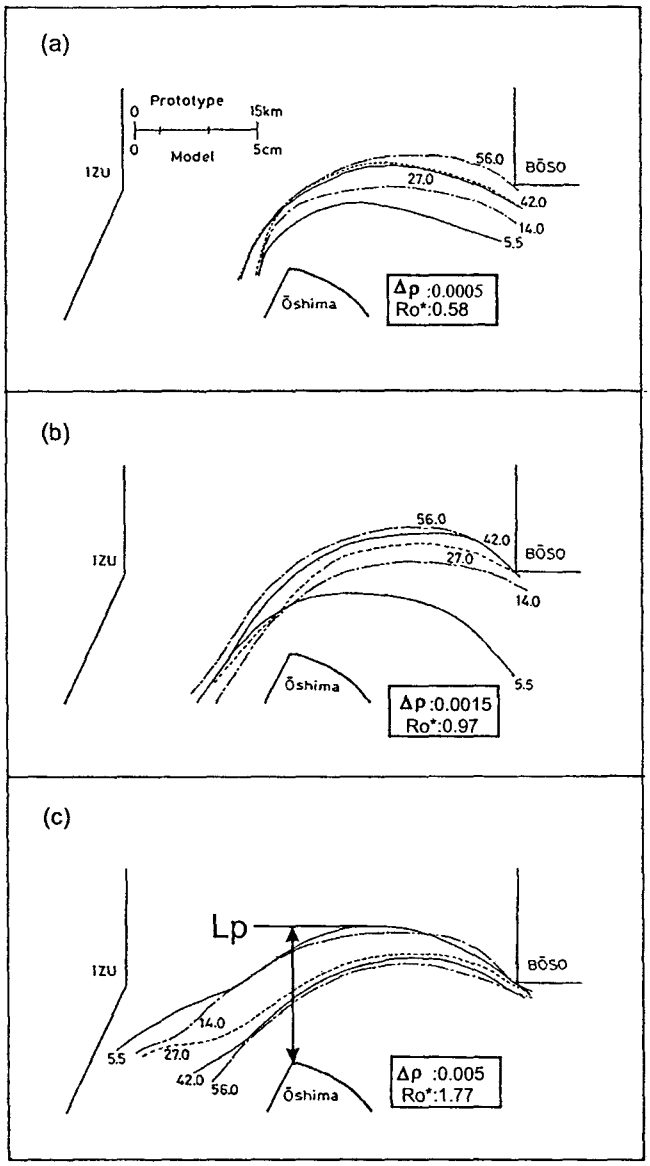

Fig. 5. Dependence of the current path on the flow rates for (a) $\Delta\rho=0.5\times10^{-3}$, (b) $\Delta\rho=1.5\times10^{-3}$ and (c) $\Delta\rho=0.5\times10^{-2}$ under 2 rpm. Lines indicate the northern boundaries of main stream.

for $Ro^*\leq1.0$ and for $1.0<Ro^*<2.0$ and rpm $\Omega=2\sim4$, Lp/L increases $1.5\times10^{-1}\sim3.0\times10^{-1}$ quickly. However for $Ro^*\geq2.0$, lp/L has little change ($3.0\times10^{-1}\sim3.5\times10^{-1}$). For Fri<1.0 (Fig. 6(b)), lp/L changes from 1.0×10^{-1} to 2.5×10^{-1}. For $Ro^*\leq1.0$, lp/L in-creases from 1.0×10^{-1} to 2.5×10^{-1} and for $Ro^*>1.0$, it has no change. For Fri=1.0 (Fig. 6(c)), lp/L has the value of $2.0\times10^{-1}\sim3.0\times10^{-1}$ and increases $2.0\times10^{-1}\sim3.0\times10^{-1}$ for $Ro^*\leq1.0$. However, for $Ro^*>1.0$, it decreases $3.0\times10^{-1}\sim2.5\times10^{-1}$. The northward penetration length rate is altered at $Ro^*=1.0$. These are identical with the results in Fig. 5 (a), (b) and (c) which show that the pattern of the Through Flow path is changed at internal Rossby number $Ro^*=1.0$.

Fig. 7(a), (b) and (c) show the contours of lp/L for density difference $\Delta\rho=2.5\times10^{-2}$ (Fri≪1.0), $\Delta\rho=1.5\times10^{-3}$ (Fri<1.0) and $\Delta\rho=5.0\times10^{-5}$ (Fri=1.0), respectively. The dotted and solid lines in figures represent the contours of external Rossby number Ro and lp/L. Fri has the range of $1.2\times10^{-2}\sim1.3\times10^{-1}$ in Fig. 7(a), $5.0\times10^{-2}\sim5.3\times10^{-1}$ in Fig. 7(b) and $2.7\times10^{-1}\sim2.89$ in Fig. 7(c). For Fri≪1.0 (Fig. 7 (a)), lp/L decreases from 3.25×10^{-1} to 2.25×10^{-1} with increase of Ro For $\Omega=1/2$ rpm and Ro<0.25, lp/L is reduced from 3.25×10^{-1} to 2.75×10^{-1} and becomes constant lp/L=0.25 for Ro≥0.25. For Fri< 1.0 (Fig. 7(b)), lp/L increases from 1.25×10^{-1} to 3.0×10^{-1} for Ro<0.25 and decreases from 3.0×10^{-1} to 2.25×10^{-1} for Ro≥0.25. For Fri=1.0 (Fig. 7(c)), lp /L increases from 5.0×10^{-2} to 2.25×10^{-1} for Ro< 0.25 and has no change with the constant value of about 2.5×10^{-1} for Ro≥0.25.

These results mean that the Through Flow paths are altered at Ro=0.25. That is, when Fri≪1.0 (Rd is wider than the breadth of Through Flow, Fig. 7 (a)), the Through Flow path descends toward Oshima Island (the decrease of lp/L) with increase of Ro except for Ro≥0.25. For Fri~1.0 (Fig. 7(c)), as Ro increases to 0.25 the Through Flow path goes up north (the increase of lp/L) except for Ro>0.25.

2. The pattern of the inner circulation

Fig. 8(a), (b) and (c) show the current vectors for density difference $\Delta\rho=1.5\times10^{-3}$ ($Ro^*=0.97$) and the flow rates of the upper layer $Q=5.5\,cm^3s^{-1}$ (Ro =0.02), $Q=27.0\,cm^3s^{-1}$ (Ro=0.11) and $Q=42.0\,cm^3s^{-1}$ (Ro=0.17), respectively. On the other hand, Fig. 9 (a), (b) and (c) indicate the current vectors for $\Delta\rho=5.0\times10^{-3}$ with the same flow rates. Arrows in each figure were drawn by tracing a water particle during 20 seconds (for $Q=5.5\,cm^3s^{-1}$), 10 seconds ($Q=27.0\,cm^3s^{-1}$) and 5 seconds ($Q=42.0\,cm^3s^{-1}$), respectively.

In Fig. 8(a) ($Ro^*<1.0$ and Ro=0.02), the model has three different currents. The first is the Through Flow that flows from the approaching channel (Oshima Western Channel) and then flows clock-

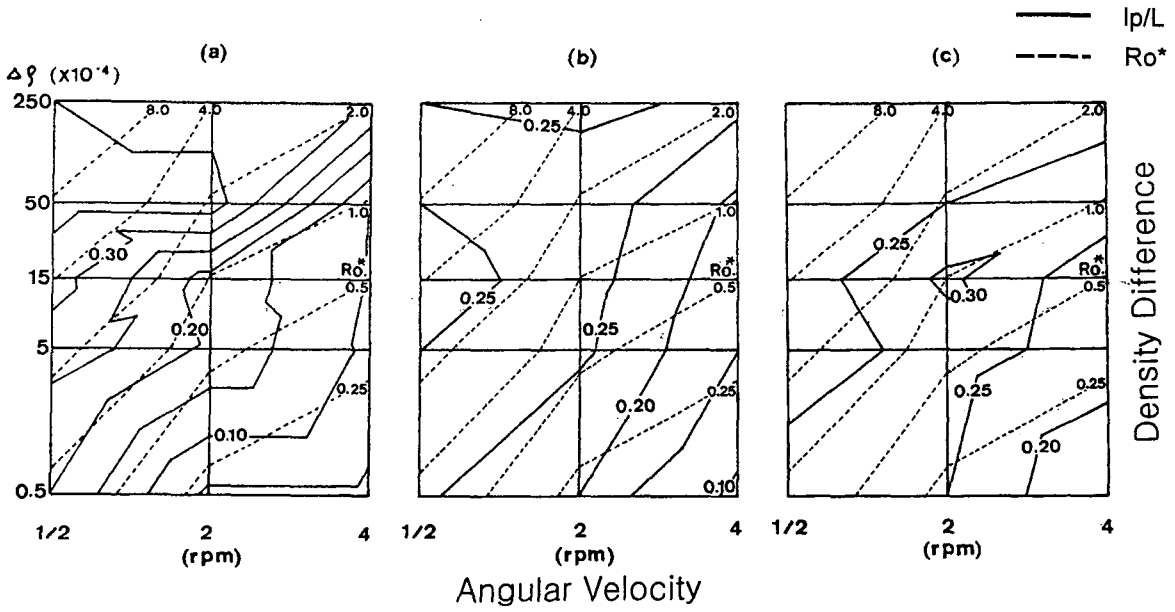

Fig. 6. Dependence of inward penetration rate lp/L of the Through Flow on internal Rossby number $((\Delta\rho/\rho)gh)^{1/2}/fB$; (dotted lines) and on corresponding flow rates for (a) Q=5.5 cm³/s, (b) Q=27 cm³/s and (c) Q=56 cm³/s. lp and L indicate the inward penetration length of the Through Flow and the horizontal length of the bay. B denotes the breadth of the entrance channel.

wise along the northern coast of Oshima Island. The second is the cyclonic circulation which exists in the inner coastal water on the north of the Through Flow. The third is an anticyclonic circulation in the most inner part of the bay detached from the north of the cyclonic circulation. Fig. 8(b) shows that the cyclonic circulation is extended to the inner bay except some northwestern parts. In Fig. 8(c), however the cyclonic circulation extends to the whole inner bay. However, Fig. 9(a), (b) and (c) show well developed cyclonic circulations in the inner part of the bay, respectively.

To examine intensity of the cyclonic circulation and effect of the eastern boundary of the bay, northward penetration length rate of the cyclonic circulation lp_c/L (lp_c, the length from the entrance of the bay to the northern boundary of the cyclonic circulation) and Rc/BE (Rc; the radius of the curvature for the cyclonic circulation, which was measured from the geometrical mean body of the cyclonic circulation, BE; the breadth of Oshima Eastern Channel) were calculated for Ro*<1.0 (0.09 ~0.74) and Ro*>1.0 (1.97~16.6), respectively and shown in Fig. 10(a) and (b). In Fig. 10(a) and (b), left and right coordinates of y axis represent lp_c/L and Rc/BE, respectively and x axis represents Ro. Symbols of open circles and black triangles show the distributions of lp_c/L and Rc/BE accor-ding to Ro. lp_c/L rises to 1.0 as Ro increases. When lp_c/L is 1.0, Ro is 0.25 in Fig. 10(a) and 0.06 in Fig. 10 (b). Also, Rc/BE increase with the increase of Ro. But when lp_c/L is 1.0, Rc/BE become to 1.0 in both Fig. 10(a) and (b). For Ro>0.25, Rc/BE are little changed with the values of 1.25~1.37 in both figures. For Ro<0.12 (lp_c/L<0.5) in Fig. 10(a), both the cyclonic circulation and the anticyclonic circulation exist in the bay (shown in Fig. 8(a)). For Ro=0.12~0.24 (lp_c/L>0.5), the cyclonic circulation gradually grows up (shown in Fig. 8(b) and (c)). Fig. 10(b) for Ro<0.6 show that the flow pattern is similar to those of Fig. 9(a) and an anticyclonic circulation exists in the inner northwestern part of the bay. While for Ro=0.60~0.24, it is shown that a well developed cyclonic circulation exists in the whole of the bay.

Discussion

1. **Dependence of northward penetration length and curvature of the Through Flow on Ro and Ro***

It has been known that the factors such as volu-

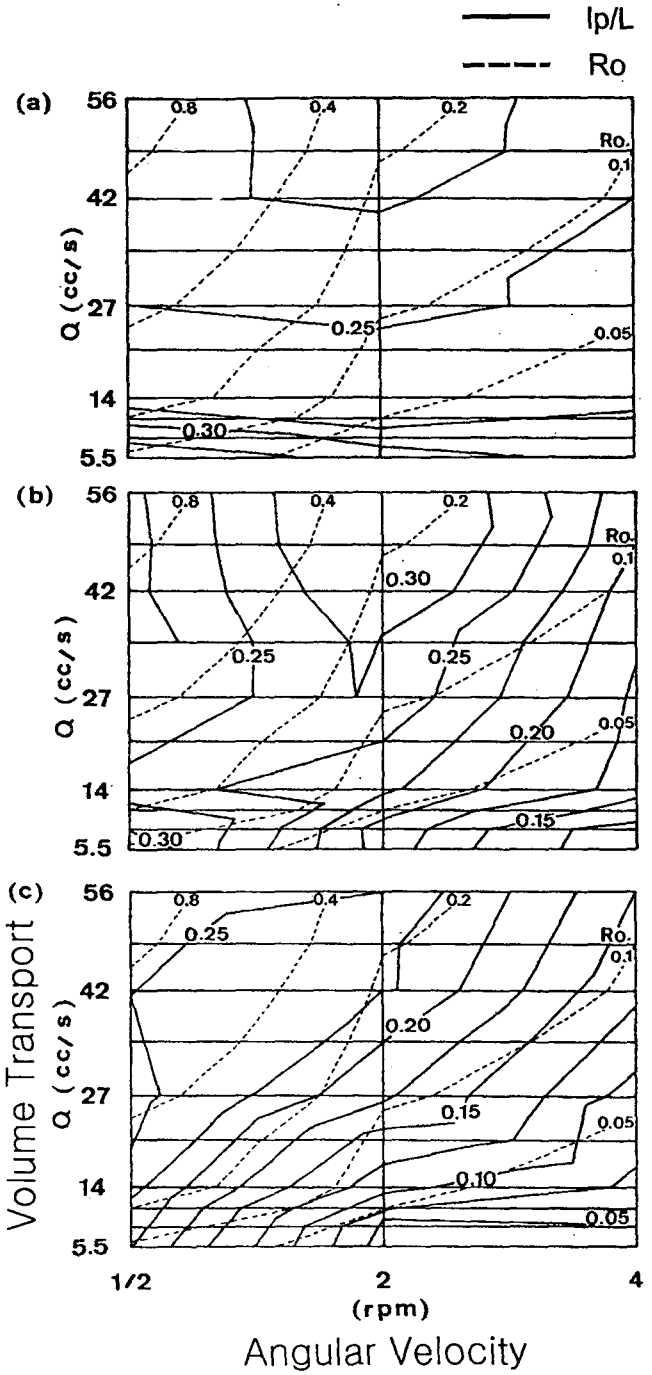

Fig. 7. Dependence of inward penetration rate lp/L of the Through Flow on Rossby number V/fL; (dotted lines) and on corresponding density differences for (a) $\Delta\rho = 0.25\times10^{-1}$, (b) $\Delta\rho = 0.15\times10^{-2}$ and (c) $\Delta\rho = 0.5\times10^{-4}$. V indicates the speed of the Through Flow.

me transport of Through Flow, density stratification, Coriolis parameter and thickness of the upper mixed layer may influence on the flow pattern in Sagami Bay. The Through Flow has anticyclonic curvature and a loop shaped path. It flows from the Western Channel of Oshima Island, which has been known as the main entrance of Kuroshio warm water. The average depth and width of Oshima Western Channel are 400 m and 21 km respectively and the latter is almost the same scale as Rossby radius of deformation of the Through Flow. If the Rossby radius of deformation of the Through Flow is not larger than the width of the channel, density front is formed in the Through Flow. In such a case, the Through Flow flows along the right-hand boundary of the approaching channel like a coastal boundary current without being aware of the left-hand boundary. The velocity shear is found at the density front between Kuroshio warm Through Flow and coastal water in the approaching channel. However, flows which are not accompanied by a density front in the approaching channel (the Rossby radius of deformation of the Through Flow is larger than the width of the channel) show the same flow pattern as those of barotropic mode (Choo and Sugimoto, 1992).

Fig. 11(a) and (b) indicate that the dependence of northward penetration length lp/L and curvature Rc^{-1} of the Through Flow on Ro*, Ro and Fri for all experimental cases. The abscissa and ordinate represent Ro and Ro*. The dotted lines in the figures are contours of Fri calculated by Ro//Ro*. The lp/L increase in company with the increase of Ro* and Ro for Ro*≤1.0 (Fig. 11(a)). Ro* in which the lp/L have maximum values are 1.7 for Ro≤0.06 and about 1.0 for Ro>0.06. Rc^{-1} decrease with Ro* before Ro* is about 1.0 (Fig. 11(b)). But For Ro*>1.0, Rc^{-1} has no change. Whitehead and Miller (1979) simulated the outflow of low density water by using a source-sink flow in a two-layer model and showed that the width of the low density water was gradually increased (It means that the width of the low density water on the right-hand side of the approaching channel is extended to the left-hand side) until its radius of deformation has come to the breadth of the approaching channel. However, when the radius of deformation for the low density water come to the breadth of the approaching channel, the low density water is changed into a jet flow.

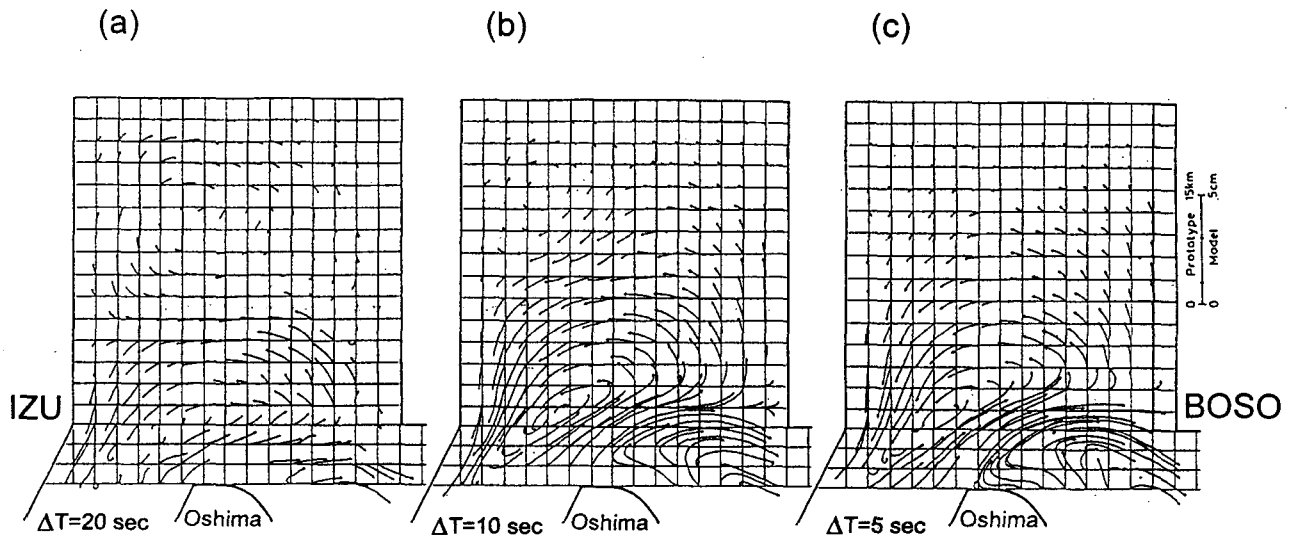

Fig. 8. Distributions of the current vectors for $\Delta\rho=0.15\times10^{-2}$, (a) Q=5.5 cm^3/s, (b) Q=27 cm^3/s and (c) Q=42 cm^3/s. Current vectors are estimated during Δt time period on each flow rate.

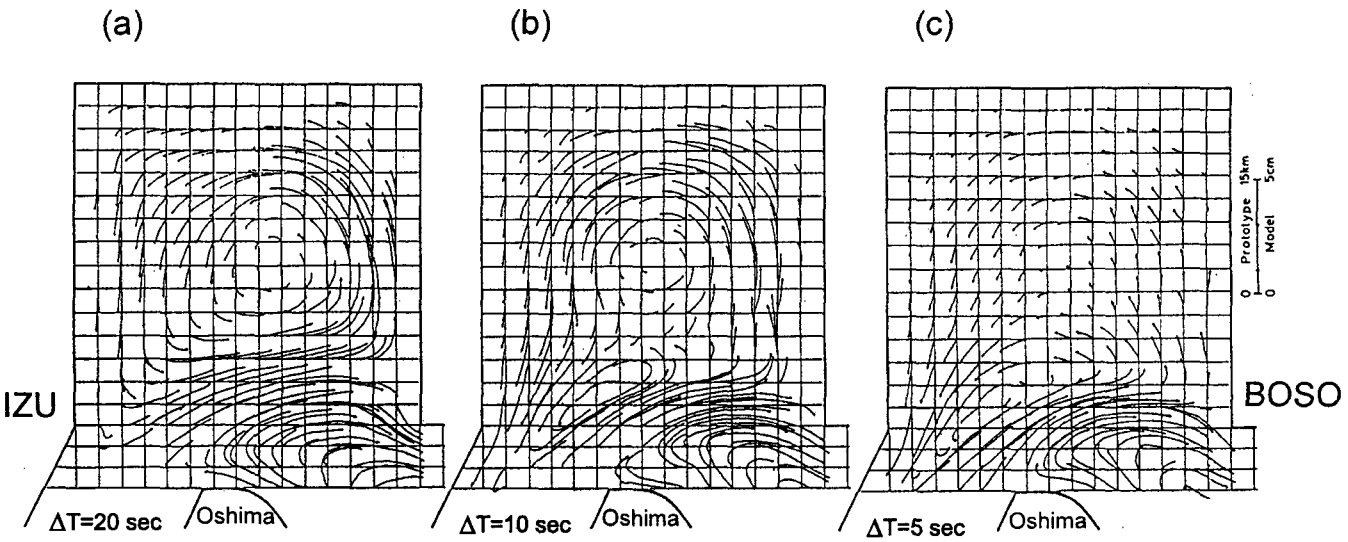

Fig. 9. Distributions of the current vectors for $\Delta\rho=0.5\times10^{-2}$, (a) Q=5.5 cm^3/s, (b) Q=27 cm^3/s and (c) Q=42 cm^3/s. Current vectors are estimated during Δt time period on each flow rate.

For Ro*>1.0, lp/L and Rc^{-1} decrease with Ro. But no change is shown for Ro>0.25. Also for Ro*≤1.0, it is shown that there is no change in flow pattern for Ro>0.25. It means that the loop shape Through Flow is able to penetrate to a half length of the bay (L/2) as Ro increase up to 0.25 (Ro=0.25 means $V/\Omega=L/2$), which is a topographic condition for the Through Flow to penetrate into Sagami Bay, and for Ro>0.25 the path of the Through Flow is not changed. Practically, the measured Rc^{-1} for Ro=0.25 has the values of 0.12 cm1 for Ro*≤1.0 and 0.1 cm^{-1} for Ro*>1.0, which mean that Rc^{-1} are less than $(L/2)^{-1}$cm^{-1} ($\sim$0.13 cm^{-1}). The reason why Rc^{-1} are less than the reciprocal of a half length of the bay $(L/2)^{-1}$ is there may be an angle of incidence 25° (measured anticyclonic from north) between the approaching channel and the bay.

In case of low Reynolds number, the Through Flow flows with the width of its own Rossby radius of deformation after flowing out from the appro-

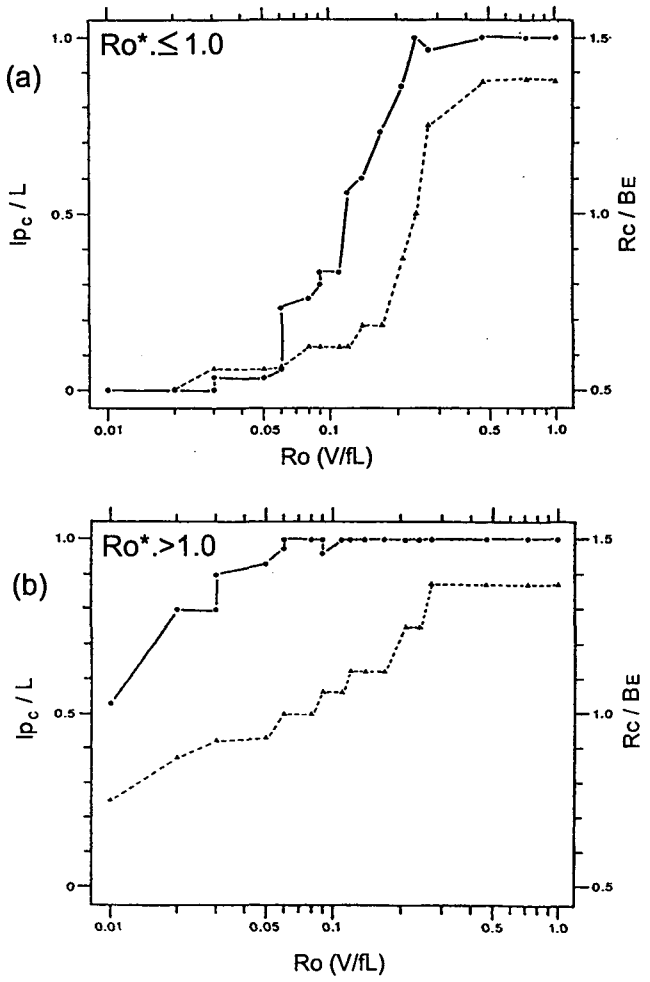

Fig. 10. Inward penetration rate lp_c/L of the inner cyclonic circulation and the effect of the eastern boundary of the bay Rc /BE (Rc; the radius of the curvature for the cyclonic circulation, BE; the breadth of Oshima Eastern Channel) on Rossby number V/fL according to the internal Rossby numbers (a) Ro*≤ 1.0 and (b) Ro*>1.0. In figures, symbols of open circles and black triangles show the distributions of lp_c/L and Rc /BE according to Ro, respectively.

aching channel. Because the curvature from the end of the approaching channel (the Western Channel of Oshima Island) to the entrance of the outflow (the Eastern Channel of Oshima Island) is about two-third of the width of the approaching channel, if the Through Flow's radius of deformation is within the range of its curvature, the Through Flow maintains a shape of coastal boundary current even within the bay. Whereas, if the radius of deformation exceeds its curvature, the Through Flow is separated from the northern edge of Oshima Island and eddies are formed at northeast of Oshima Island. The origin of these eddies are identical with the formation of warm eddies by Whitehead and Miller (1979)'s hydraulic model experiments.

Meanwhile, the Reynolds number increases and from its medium stage, the Through Flow leaves from the northern part of Oshima Island regardless of the radius of deformation. This is a generating process of topographical eddies (wakes) formed at the lee side of cylindrical objects. Baines and Davis (1980) showed those eddies were dependent on Ro and Ek ($Ek=\nu/2\Omega L^2$, ν; molecular viscosity of the model fluid). When the radius of deformation is two-third of the width of the Western Channel of Oshima Island ($Ro^*=0.66$), the curvature of the Through Flow is about 0.2 cm^{-1} for Ro=0.01 (Fig. 11(b)), which corresponds to the curvature in northern parts of Oshima Island. Fig. 11(b) shows a sudden decrease of the curvature from $Rc^{-1}=0.20$. Ro=0.12 for $Rc^{-1}=0.20$ is the experimental case that the cyclonic circulation starts to grow, which has been shown in the distributions of lp_c/L in Fig. 10(a).

In our model experiments, the accurate Ek were not obtained. For an appropriate Ek, the value of 0.42 rad/sec for revolution rate Ω and the radius of Oshima Island (5 cm) for length scale L were given and about 10^{-3} was obtained. Thus, according to Baines and Davis (1980), our results for Ro=0.12 and $Ek\sim10^{-3}$ are corresponding to the experimental stages just after eddies have been formed at the lee side of a cylindrical object.

2. Dependence of circulation pattern on non-dimensional parameters

There are many studies that a linear shallow water equation is used for analysing the frontal genesis of low density water by the approximation that the propagation speed of low density water is much slower than that of gravity wave. It has been known that in case of no continuous inflow from a source, the eddies by baroclinic instability or shear velocity at a density front were dependent on Fri ($(Lo/Rd)^2$) (Griffith and Linden, 1982; Chia et al., 1982). From one-layer hydraulic model experiments in Sagami Bay (Choo and Sugimoto, 1992), it was found that cyclonic circulations were caused by wakes. Mean-

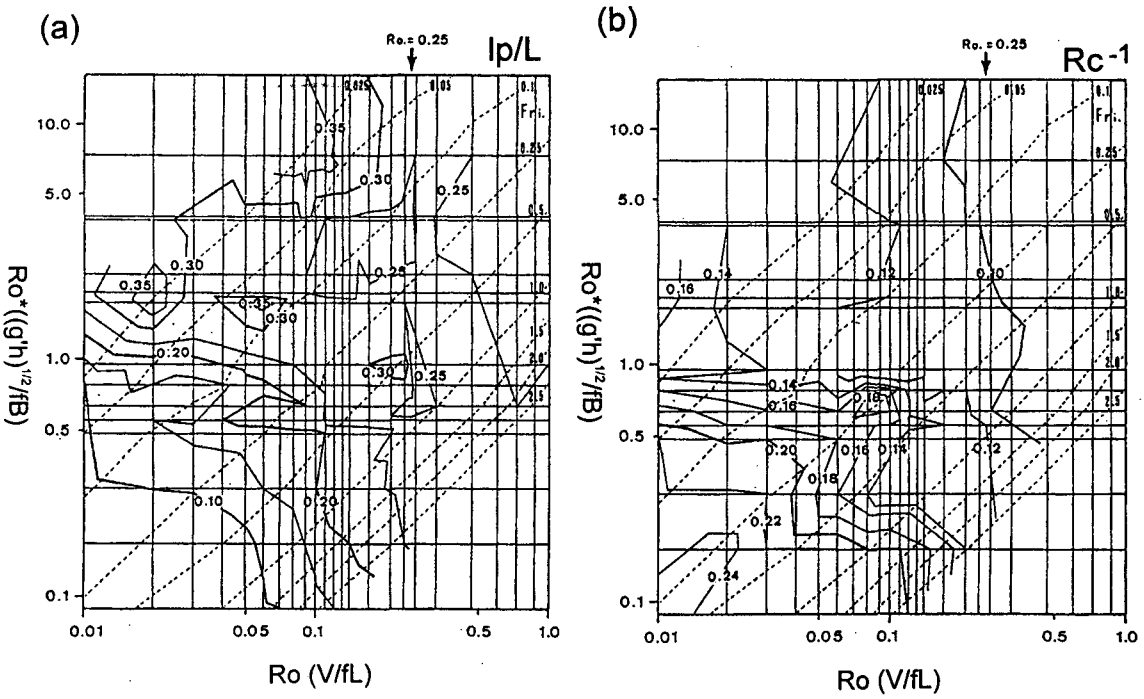

Fig. 11. (a) Inward penetration rate lp/L and (b) curvatures Rc^{-1} of the Through Flow on internal Rossby number $((\Delta\rho/\rho)gh)^{1/2}/fB$ and Rossby number V/fL in all cases of the two layer model experiment.

while, in our two-layer model experiments, several patterns of circulations were in existence.

For Ro*<1.0 (Fig. 8(a)), it was confirmed that eddies or wavelike current vectors appeared in the frontal regions between the Through Flow and the cyclonic circulation. Also, the cyclonic circulation was formed and maintained by eddies and frontal wave streamers from the frontal regions. Meanwhile, the anticyclonic circulation was formed by anticyclonic vorticity supplied at the northern boundary of the cyclonic circulation until the cyclonic circulation extends to the breath and the half length of the bay. The anticyclonic circulation gradually died out when the Through Flow penetrated into the bay and the cyclonic circulation grew more and more (Fig. 8(b) and (c)).

As Rossby internal radius of deformation for Through Flow is larger than the breath of the approaching channel (Ro*>1.0), the cyclonic circulation caused by topographical wakes was built up. In Fig. 9(a), the center of the cyclonic circulation is located at the eastern part of the bay under the influence of the frontal wave streamer. In Fig. 9(b) and (c), the cyclonic circulation is developed by cyclonic vorticity from the outskirts of the cyclonic circulation.

Table 3 shows the patterns of cyclonic circulation based on non-dimensional parameters in our model experiments. Frontal wave streamer (FWS) is a sort of disturbance occurring from one or more than two instabilities synthetically in the frontal area (Fig. 12 (b)) and can be described by both Ro $((V_1-V_2)k/2f$, V_1, V_2; upper and lower layer speeds, k; wave number) and Ri $(g'h/(V_1-V_2)^2)$ (Olanski, 1968). The circulation pattern of FWS (I) in Table 3 represents that the detrained unsteady state eddy rows (keeping the cyclonic vorticity) from the Through Flow form the FWS in the inner part of the bay. Stern et al. (1982) pointed out that such a FWS was principally formed by long-term density (vorticity) diffusion (conservation of potential vorticity) and formed by propagation of a coastal boundary current as a secondary effect. Meanwhile, Stern (1985) and Stern and Pratt (1985) suggested that a FWS was formed in the process that an early disturbance of finite amplitudes occurring from fronts and low vortical surrounding waters grew up and disappeared with time, which was equivalent to the process that the disturbing energy was transferred to a mean flow (kinetic energy).

Table 3. The type of inner part circulations in accordance with non-dimensional parameters on the baroclinic experiments

Type	The conditions of non-dimensional parameters	The pattern of inner circulation
1) FWS (I)	Ro*≤1.0 , Ro<0.12	cyclonic and anticyclonic cir.
2) FWS (II)	Ro*≤1.0 , 0.12≤Ro<0.25	The growth of cyclonic cir.*
3) FWS-CBC	Ro*≤1.0 , Ro≥0.25	full development of cyclonic cir.**
4) FWS (I)-Wake	Ro*>1.0 , Ro<0.06	the growth of cyclonic cir.*
5) FWS (II)-Wake	Ro*>1.0 , 0.06≤Ro<0.25	full development of cyclonic cir.
6) FWS-CBC-Wake	Ro*>1.0 , Ro≥0.25	occurrence of coastal boundary current on eastern boundary of bay

*anticyclonic circulation on some inner part.
**occurrence of coastal boundary current on eastern boundary of bay.

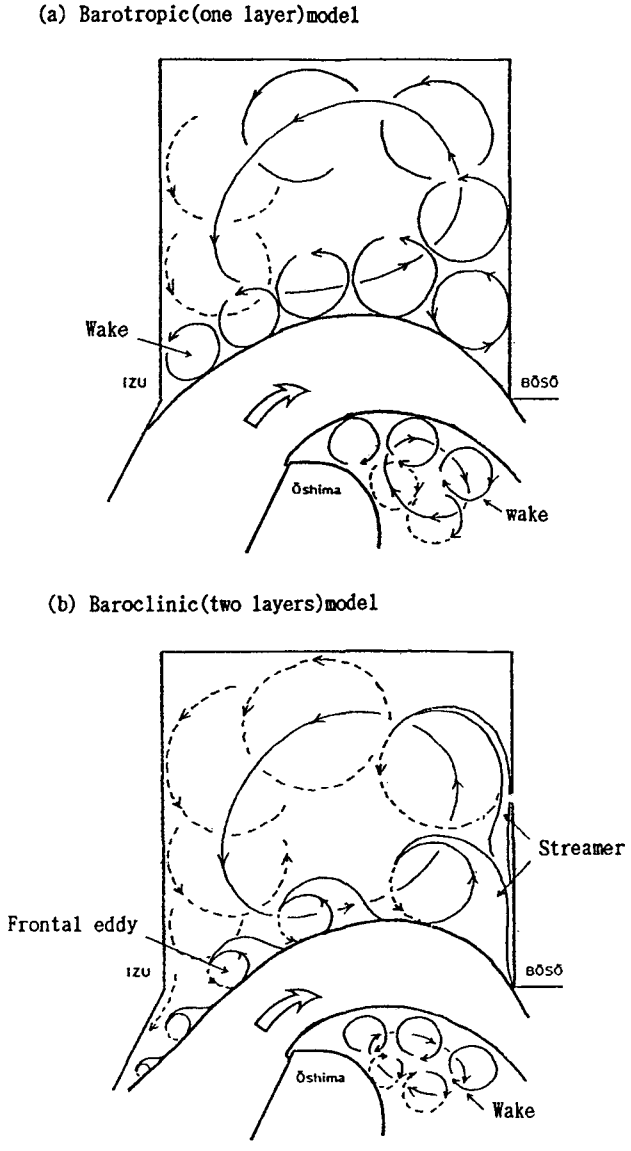

Fig. 12. Schematic views of the inner cyclonic circulation created or preserved by (a) wake and (b) frontal eddies or streamers.

FWS (I) indicates the circulation pattern for Ro< 0.12 (Fig. 8(a)), and the center line of the detrained eddy rows from the Through Flow does not reach the eastern boundary. On the other hand, FWS leaves from the stagnation point at the western boundary and forms an anticyclonic circulation in the inner side of the model bay.

FWS (II) in Table 3 indicates the circulation pattern for 0.12≤Ro<0.25 (Fig. 8(b)), so that the inertial force on the circulation of FWS (II) is greater than that of FWS (I). The center line of eddy rows (after this, vorticity front; Stern (1985)) reaches the eastern boundary. As the non-slip condition is identical with the condition that FWS should move up north along the eastern boundary, circulations in the inner side of the model bay are gradually changed to a cyclonic circulation by FWS from the eastern boundary.

As the inertial force become more and more increased (Ro>0.25, (Fig. 8(c)), the circulation pattern of FWS-CBC in Table 3 shows that a coastal boundary current (CBC) is formed from the Through Flow and flows along the eastern boundary. Then, CBC circulates the model bay anticlockwise and FWS is formed from the left-hand edge of CBC. Flows in the model become complicated for the interaction of FWS and CBC. However, there exists a fast cyclonic circulation in the model.

In case of low external Rossby number (Ro<0.6, Fig. 9(a)), FWS from the Through Flow is extended to the eastern boundary and transported to the inner bay. As the vorticity front corresponds to non-slip condition at the eastern boundary, going up north of FWS from the Through Flow is remarkable (FWS (I)-Wake).

As, for $0.6 \leq Ro < 0.25$ (Fig. 9(b)), the Through Flow is separated from the western boundary of the approaching channel, the vorticity front come down and the circulation pattern begin to be much of the same as FWS (II). Moreover, as the wake strengthens gradually, the circulation develops into a pattern in Fig. 9(a) and (b) (FWS (II)-Wake). In case of $Ro > 0.25$ (Fig. 9(c)), both CBC and wakes occur, and flows in the model show a large cyclonic circulation (FWS-CBC-Wake).

3. Comparison of the model experiments and field observations

In our baroclinic model experiments, the Through Flow, the cyclonic circulation in the inner part of the bay and the wake on the northeast of Oshima Island were simulated. From both barotropic (Choo and Sugimoto, 1992) and baroclinic model, it is found that the circulation pattern is strongly depended on the volume transport and the density difference between the upper and the lower layer of the Through Flow.

Choo (1992) investigated the relation between the calculated volume transport of the Through Flow in Oshima Western Channel and the current direction (path of the Through Flow) by long period current observations in Sagami Bay. The calculated volume transport ranged from 2.2 Sv to 4.1 Sv during the current observations, which approximately coincided with the observational results (0.5 Sv~4.0 Sv) by Teramoto (1965) and Taira and Teramoto (1986). According to the results (Choo, 1992), the current direction changed from 45° to about 90° when the calculated volume transport changed from 0.1 Sv to 1.0 Sv. The current was headed eastward (90°) and showed no change in its direction while the calculated volume transport ranged from 1.0 Sv to 4.0 Sv. These correspond to the results that the Through Flow path depends on Reynolds number and shows no change in current path for $Re \geq 540$ (0.9 Sv in prototype) in barotropic and baroclinic model experiments. From the NOAA infrared imagery analysis, Tameishi (1988) reported that when the catches of the Saury were abundant at fixed nets in Sagami Bay, the Through Flow path was along the northern boundary of Oshima Island. However, when the catches of the Saury were small, the Through Flow penetrated into the bay much further. This means that the Through Flow path was dependent upon its current velocity, that is, Reynolds number.

In baroclinic mode, the Through Flow path depends on both external and internal Rossby number. Whitehead and Miller (1979) obtained the results on the change of the flow pattern by the internal Rossby number from the hydraulic model experiments and field measurements in Alboran Sea. Those are in accord with our two-layer model experiments. Internal Rossby number is proportional to the square root of density difference between the upper and the lower layer. Therefore, the Through Flow path in Sagami Bay may be changed not only by the volume transport for inflow but also by the density difference between two layers. To intensify our discussion on the results of the two-layer model experiments, it is necessary to make a field observation on the fluctuations of the Through Flow path caused by the density difference between the surface Through Flow water and the lower subarctic intermediate water.

4. The mechanism of formation and preservation for the cyclonic circulation

The inner cyclonic circulation in barotropic model was originated by wakes which were formed between Izu Peninsula and the entrance of the approaching channel at first and transferred by the Through Flow to the eastern boundary of the bay and maintained by the continuous inflow of the wakes (Choo and Sugimoto, 1992). Fig. 12(a) shows a schematic view of the inner cyclonic circulation created and preserved by wakes in Sagami Bay. The cyclonic circulation increases with the Reynolds number and accounts for about 20 percent of the inflow for $Re \geq 540$. Nishimura et al. (1984) reported that the wakes were originated at capes by passage of the Kuroshio in southern coast of Japan from the analysis of NOAA infrared imagery. Awaji et al. (1991) executed numerical experiments using a barotropic source-sink flow model and found that the wakes made currents on the continental self when the Kuroshio was approached to the coast. Also they examined effects against the fluctuation of the Kuroshio path on the continental self. These mean that the wakes play a main role in producing a circulation caused by the strong current like the Kuroshio at the rear of coastal regions.

In our two-layer model, the pattern of the cyclonic circulation is determined by Ro and Ro*. That is, in case of Ro*≤1.0 frontal waves develope and frontal eddies and frontal wave streamers are formed at the northern boundary (the out edge) of the Through Flow. The frontal eddies and the frontal streamers flow in continuously along the eastern boundary of the bay and provide the vorticity to maintain the inner cyclonic circulation (Choo and Sugimoto, 1999). Fig. 12(b) shows a schematic view of the inner cyclonic circulation created and preserved by the frontal eddies and the frontal streamers in Sagami Bay. The pattern of the cyclonic circulation is divided into three types; 1) a cyclonic circulation and an inner anticyclonic circulation (Ro<0.12, FWS (I), Fig. 8(a)), 2) an only cyclonic circulation in the bay (0.12≤Ro<0.25, FWS (II), Fig. 8(b)), 3) a cyclonic circulation and boundary currents along the eastern boundary of the bay (Ro≥0.25, FWS-CBC, Fig. 8(c)). For Ro*>1.0, the wakes which are caused by the barotropic jet flow from the Izu peninsula flow in the inner cyclonic circulation in addition to the frontal eddies and the frontal streamers (Fig. 9(a), (b), (c)). The horizontal dimensions of the inner cyclonic circulation are determined by interaction between the Through Flow and the eastern boundary of the bay. It means that, in case that the radius of curvature of the Through Flow can not reach the width of the outflow channel (Oshima Eastern Channel), the inner cyclonic circulation is formed to the half length of the bay and an anticyclonic circulation is created in the inner part of the bay.

Studies on the formation of the frontal eddy or the frontal wave streamer have been made by Lee et al. (1981), Lee and Atkinson (1983) and Brooks and Bane (1983) by means of field observations, and by Stern (1985) and Stern and Pratt (1985) theoretically. In our hydraulic model experiments it is found that the cyclonic circulation formed by the inflow of the upper low density water is originated and maintained by frontal eddies and frontal streamers in Sagami Bay.

References

Awaji, T., K. Akimoto and N. Imasato. 1991. Numerical study of self water motion driven by the Kuroshio: Barotropic model. J. Phys. Ocenogr., 21, 11~27.

Baines, P.G. and P.A. Davis. 1980. Laboratory studies of potographic effects in rotating and/or stratified fluids. In *Orographic Effects in Planetary Flows,* R. Hide and P. White, eds. GARP Publ. Ser., 23, pp. 233~299.

Brooks, D.A. and J.M. Bane. 1983. Gulf Stream meanders off North Carolina during winter and summer 1979. J. Geophys. Res., 88, 4633~4650.

Chia, F., R.W. Griffiths and P.F. Linden. 1982. Laboratory experiments of fronts. Part 2: The formation of cyclonic eddies at upwelling fronts. Geophys. Astrophys. Fluid Dynam., 19, 189~206.

Choo, H.S. 1992. Studies on the Mechanics of Circulation and Its Fluctuation in Sagami Bay. Doctorial Dissertation, University of Tokyo, pp. 19~20.

Choo, H.S. and T. Sugimoto. 1992. Hydraulic model experiment on the circulation in Sagami Bay (1) -Dependency of the circulation pattern on Reynolds and Rossby Numbers in Barotropic rotating model-. Bulletin on Coastal Oceanography, 29, 179~189 (in Japanese).

Choo, H.S. and T. Sugimoto. 1999. Hydraulic model experiment on the circulation in Sagami Bay, Japan (IV) -The time-varing states of the flow pattern and water exchange in baroclinic rotating model-. Environmental Sciences, 3, 57~73.

Griffith, R.W. and P.F. Linden. 1982. Laboratory experiments on fronts. Part 1: Density driven boundary current. Geophys. Astrophys. Fluid Dynam., 19, 159~187.

Hasunuma, K., H. Nakada, H. Nagae and T. Hirano. 1983. Surface circulation and its fluctuation in Sagami Bay. Abstracts of Aut. Con. of Japan J. Oceanogr. 1983, pp. 13~14 (in Japanese).

Iwata, S. 1979. Mean oceanic condition in Sagami Bay. Observational Report of Fisheries Environment in Sagami Bay-2, Kanagawa Prefectural Fishery Experimental Station, pp. 15~25 (in Japanese).

Iwata, S. 1986. Studies on the short-term variations of oceanic conditions in Sagami Bay. Special Rep. of the Kanagawa Prefectural Fishery Experimental Station, 3, pp. 1~64 (in Japanese).

Iwata, S. and M. Matsuyama. 1989. Surface circulation in Sagami Bay: The response to variations of the Kuroshio axis. J. Oceanogr. Soc. Japan, 45, 310~320.

Kawasaki, Y. and T. Sugimoto. 1984. Experimental studies on the formation and degeneration processes of the Tsugaru Warm Gyre. In *Ocean Hydrodynamics of the Japan and East China Seas,* T. Ichiye, ed. Elsevier Sci. Publ., Amsterdam, pp. 225~238.

Kawasaki, Y. and T. Sugimoto. 1988. A laboratory study of the short-term variation of the outflow pattern of the Tsugaru Warm Water with a change in its volume transport. Bull. Tohoku Reg. Fish. Res. Lab., 50, 203~215 (in Japanese).

Kawata, K. and N. Iwata. 1957. Currents in Sagami Wan. Hydrographic Bulletin, Maritime Safety Board, Tokyo, Japan, 53, 44~47 (in Japanese).

Kimura, K. 1942. Kyucho event in coastal areas. Tech.

Rep. of the Central Meteorological Observatory of Japan, 19, 1~85 (in Japanese).

Kubokawa, A. and K. Hanawa. 1984. A theory of semigeostrophic gravity waves and its application to the intrusion of a density current along a coast. Part 2. Intrusion of a density current along a coast in a rotating fluid. J. Oceanogr. Soc. Japan, 40, 260~270.

Lee, T.N., L.P. Atkinson and R. Legeckis. 1981. Observations of a Gulf Stream frontal eddy on the Georgia continental shelf, April 1977. Deep-Sea Res., 4, 347~378.

Lee, T.N. and L.P. Atkinson. 1983. Low frequency current and temperature variability from Gulf Stream frontal eddies and atmospheric forcing along the southeast U.S outer continental shelf. J. Geophys. Res., 88, 4541~4567.

Momoi, K. 1976. Statistical Studies on the Surface Current in Sagami Bay and Zunan Coastal Areas. Graduation Thesis, Tokai Univ., 112pp. (in Japanese).

Nakada, H., K. Hasunuma and T. Hirano. 1989. Distribution of sardine eggs and larvae related to the surface circulation in Sagami Bay. J. Oceanogr. Soc. Japan, 45, 11~23.

Nishimura, T., Y. Hatakeyama, S. Tanaka and T. Maruyasu. 1984. Kinetic study of self-propelled marine vortices based on remotely sensed data. In *Remote Sensing of Self Sea Hydrodynamics,* J.C.J. Nihoul, ed. Elsevier Oceanography Series, Amsterdam, 38, 69~105.

Nof, D. 1978. On geostrophic adjustments in sea straits and wide estuaries: Theory and laboratory experiments. Part 2: Two-layer system. J. Phys. Oceanogr., 8, 861~872.

Odamaki, M. 1991. Currents in Sagami Bay as one of the sea bottom environment. KAIYO MONTHLY, 23, 418~423 (in Japanese).

Orlanski, I. 1968. Instability of frontal waves. J. Atmos. Sci., 25, 178~200.

Stern, M.E., J.A. Whitehead and B.-L. Hua. 1982. The intrusion of a density current along a coast of a rotating fluid. J. Fluid Mech., 123, 237~265.

Stern, M.E. 1985. Lateral wave breaking and shingle formation in large scale shear flow. J. Phys. Oceanogr., 15, 12 74~1283.

Stern, M.E. and L.J. Pratt. 1985. Dynamics of vorticity fronts. J. Fluid Mech., 161, 513~532.

Sugimoto, T. 1977. Physical oceanographical structure of the coastal boundary region of the Kuroshio. Monthly Marine Science, 9, 188~193 (in Japanese).

Taira, K. and T. Teramoto. 1986. Path and volume transport of the Kuroshio current in Sagami Bay and their relationship to cold water masses near Izu Peninsula. J. Oceanogr. Soc. Japan, 42, 212~223.

Taira, K., T. Teramoto and K. Takeuchi. 1987. Centrifugal forces estimated from trajectories of drifting buoys in winding paths of the Kuroshio. J. Oceanogr. Soc. Japan, 43, 104~110.

Tameishi, H. 1988. Fisheries of Saury and oceanic condition in Sagami Bay. Bull. Japan Soc. Fish. Oceanogr., 52, 319~323 (in Japanese).

Teramoto, T. 1965. Day-to-day to Monthly Variations in Oce-anic Flows Estimated from Cross-stream Differences in Electric Potential. Doctorial Dissertation, Univ. of Tokyo, 74pp.

Uda, M. 1937. The relation of meteorological and oceanic condition to fishery in Sagami Bay in the fishing season of Yellowtail. Res. Rep. of Fishery Experimental Station, 8, 1~59 (in Japanese).

Vinger, A. and T.A. McClimans. 1980. Laboratory studies of baroclinic coastal currents along a straight, vertical coastline. River and Harbour Laboratory Report, STF60 A80 081, 1~15.

Whitehead, J.A. and A.R. Miller. 1979. Laboratory simulation of the gyre in the Alboran Sea. J. Geophys. Res., 84, 37 33~3742.

Yoshida, S. 1960. On the short period variation of the Kuroshio in the adjacent sea of Izu Islands. Hydrographic Bulletin, Maritime Safety Board, Tokyo, Japan, 65, 1~18 (in Japanese).